YOULIANG XIE
YUZHOU FENG
JIANPING LIU
HAODI ZHOU
and
HUAJIE TAN

Mineral chemistry of W-bearing rutile: an indicator for porphyry mineralization in the Dabaoshan Mo polymetallic deposit, South China

The Dabaoshan Mo-polymetallic deposit is located in the Nanling Metallogenic Belt, China. It consists of porphyry Mo, skarn Mo and strata"-bound Cu–Pb–Zn mineralization, of which rutile was only found in potassium feldspar alteration zones surrounding porphyry Mo orebodies. Petrographic observation combined with in–situ major elements mapping analysis by EPMA show that there are two generations of rutile, namely rutile I and rutile II. Rutile I with larger grain sizes(approximating to 100×200 μm^2) occur closer to the mineralization center of porphyry Mo orebodies than rutile II with smaller grain sizes(nearly 20×15 μm^2). Besides, rutile I grains are chemically zoned (in W and Cr), while rutile II are less likely to show chemically zoning. Rutile I grains have high W contents (4.79–9.57 wt%) and Cr contents (2.24–3.09wt%) in coherent zones. Slower diffusion rate on crystal face of W6+, which is the cation with the highest chemical valence and smallest radius, is an important factor accounting for chemical zoning in rutile I. Above all, the rutile in biotite and K–feldspar alteration zones surrounding porphyry Mo orebodies, especially those with large grian sizes,W-Cr anomaly and chemical zoning, are critical indicator of economic mineralization and mineralization center.

Keywords: *W-bearing rutile, EPMA, Dabaoshan, South China*

1. Introduction

Rutile is an accessory mineral commonly occurring in metamorphic rocks, igneous rocks, mantle-derived xenoliths, lunar rocks, meteorolite, and multiple metallic mineral deposits. It is an important titanium minerals dominated by TiO_2. Though with good chemical stability, rutile usually has isomorphic replacement elements entering its crystal lattice, including W^{6+}, U^{6+}, Nb^{5+}, Ta^{5+}, Sb^{5+}, Zr^{5+}, Mo^{4+}, Sn^{4+}, Hf^{4+}, U^{4+}, Fe^{3+}, Al^{3+}, Se^{3+}, Y^{3+}, Cr^{3+}, V^{3+}, Mg^{2+}, Zn^{2+}, and Mn^{2+} [1–10].

A large number of previous literatures have mentioned rutile in porphyry Cu (–Mo or –Au) deposits. Lawrence and Savage (1975) [11] described the occurrence of rutile in porphyry Cu-Mo deposits in Melanesia and the United States. Williams et al. (1977) [12] compared Cu contents of rutile from a number of porphyry Cu (–Mo or –Au) deposits and other geological environments, and all porphyry–related rutile samples has Cu contents ranging from 100 ppm to 500 ppm, while no rutile of other origin has Cu contents exceeding 50 ppm. Besides, the Cu content decreases with increasing distance from the center of the porphyry Cu mineralization system. Czamanski et al. (1981) [13] studied on the relationship of rutile crystallization, Cu ore grade and alteration assemblage, and found that rutile abundance and grain size were obviously consistent with Cu ore grade, and the physico-chemical conditions of potassium feldspar alteration also enhance rutile crystallization. Compared to TiO_2 content, the type of alteration was more important to rutile abandance in a porphyry deposit. Scott (2005) [9] measured the composition of rutile from Cu–Au deposits in the Northparkes district, central-western New South Wales, Australia by the wavelength-dispersive electron microprobe, and found that the rutile close to orebodies were enriched in V (commonly >0.4%), while those barren rutile distal to orebodies generally contained <0.15%. Li et al. (2008) [14] found that the V contents of rutile could be an indicator to locate the scope of main orebodies, by studying the composition of rutile in ores from the Duobuza porphyry Cu–Mo deposit in Tibet using electron microprobe.

The Dabaoshan Mo-polymetallic deposit is the largest porphyry Mo deposit hosted in the Nanling Metallogenic Belt, containing 52,000 metric tonnes (t) Mo metal [15-16]. A number of studies have been done on geological and geochemical characteristics including geology setting, geology of the deposit, rock and ore–forming ages and genesis [17-21]. However, no studies have been carried out on composition and mineral indicator of rutile in the deposit.

Messrs. Youliang Xie, Jianping Liu, Haodi Zhou, Huajie Tan, School of Geosciences and Info-Physics, Central South University, Changsha 410083, and Yuzhou Feng, Key Laboratory of Mineralogy and Metallogeny, Guangzhou Institute of Geochemistry, Chinese Academy of Sciences, Guangzhou, 510640, China. Email: 747958257@qq.com

Content variation of isomorphic replacement elements is helpful for understanding precipitation process of rutile and physico-chemical condition changes during the process. Besides, content variation of isomorphic replacement elements in rutile from porphyry Cu (–Mo or –Au) deposits has been identified as an available indicator for mineral prospecting. This study aims at building a mineral indicator for porphyry Mo mineralization in the Dabaoshan Mo-polymetallic deposit by analyzing chemical compositions of rutile utilizing EMPA.

2. Geological setting

2.1 Regional geology

The Nanling Metallogenic Belt (NLMB), at the southeast region of the Cathysia Block [16], is famous for its extensive mesozoic granitic magmatism and related mineralization. It contains more than 50% of the world's tungsten reserves, 20% of the world's total tin reserves and several important copper and molybedenite deposits, with the Shizhuyuan district hosting the largest skarn Cu–Pb–Zn deposit and the Dabaoshan district hosting the largest porphyry Mo deposit in the region [15-16, 22]. Sedimentary rocks, comprising paleoproterozoic sandstone, Ordovician shale formation, upper Devonian to Triassic carbonate and clastic rocks, Neogene clastic rocks and Quaternary soil, extend in NW and NNW direction in the region. The NLMB underwent multiple episodes of tectonic movements from proterozoic to mesozoic. The dominant periods are marked by Caledonian, Indosinian and Yanshanian. As a result, the region is characterized by complex folds and faults, such as the XueShanzhang anticline, Wengcheng and Beijiangsyncline, Wuchuan–Sihui and Dadongshan–Guidong deep faults. Corresponding to the tectonic movement, the NLMB underwent multiple episodes of granitic magmatism from proterozoic to mesozoic, dominated by Caledonian, Indosinian and Yanshanian periods, and the metallogenic events are mainly related to mesozoic magmatism. As a consequence, a magmatic belt, comprising the Jiufengshan–Zhuguangshan, Dadongshan–Guidong and Fogang plutons, extends from north to south. A large number of Mo-polymetallic porphyry deposits, Cu polymetallic skarn deposits, magmatic hydrothermal Cu-Pb-Zn polymetallic deposits and weathering–infiltration Fe deposits are genetically related to Yanshanian granites. Among those deposits, the Dabaoshan mo-polymetallic deposit is a large deposit with better quality and well–developed, constituting a typical example for understanding porphyry Mo mineralization in northern Guangdong.

2.2 Deposit geology

2.2.1 Stratigraphy

The Dabaoshan district lies in the intersection of the N-trending Dadongshan-Guidong tectono-magmatic belt and the NE-trending Sihui-Wuchuan fault, which was in the middle segment of the Nanling Metallogenic Belt (Fig.1). The strata of the Dabaoshan deposit is mainly composed of the Cambrian meta-sandstone of Gaotan formation in the northwestern area of the district, the Mid-Devonian limestone of Donggangling formation in the eastern area of the district, the Upper Devonian limestone of Tianziling formation in the western area of the district, and the Lower Jurassic gray wackes and shales of Jinji formationin in the southwestern area of the district. The Mid-Devonian limestone of Donggangling formation can be subdivided into two parts. The lower subdivision, consisting of carbonaceous mudstone and dolostone, is the main host for strata-bound Cu-Pb-Zn mineralization. The Upper Devonian Tianziling formation, consisting of moderate–to thick–layered micitic limestone intercalated with thin-layered, micritic limestone, is the dominant host for Mo skarn mineralization.

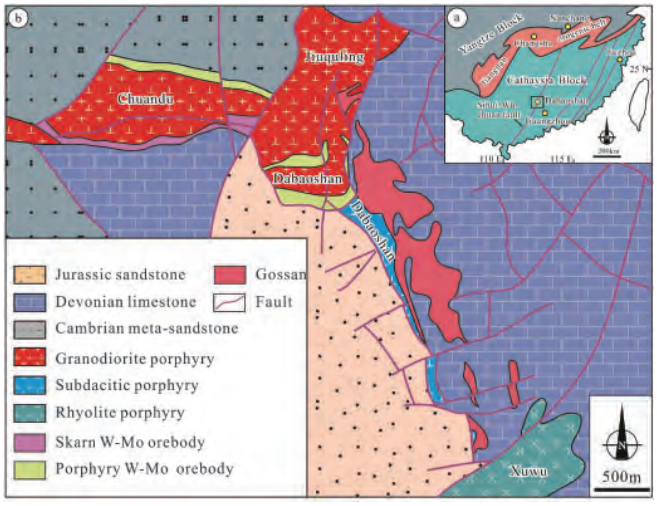

Fig.1 (a) Tectonic maps indicating the location of the Dabaoshan Mo-polymetallic deposit, Southern China; (b) Geological map of the Dabaoshan Mo-polymetallic deposit (modified after Zhu et al., 2011[23]).

2.2.2 Igneous Rocks

There are two episodes of intrusive magmatism in the Dabaoshan district. The early intrusion is the Xuwu dacite porphyry, of which SHRIMP zirconU-Pb ages of 441Ma was obtained [24]. The late intrusions contain the Chuandu granodioritic porphyry, Dabaoshan granodioritic porphyry and the Jinquling dacitic porphyry, of which LA-ICP-MS zircon U-Pb ages of 160Ma, 161Ma and 162Ma were obtained respectively [14]. The Jurassic Chuandu granodioritic porphyry display fine"medium grained texture and massive structure, consisting of plagioclase (45%), feldspar (20%), quartz (25%), biotite (8%) and minor muscovite and magnetite. The Dabaoshan granodioritic porphyry has porphyaceous texture and massive structure, and the phenocrysts are composed of quartz (10%) and feldspar (5%). The Jurassic Dabaoshan and Jinquling dacitic porphyry have porphyaceous texture and massive structure, and phenocrysts are composed of 20% plagioclase, 20% quartz, 5% biotite and 5% feldspar. The Silurian Xuwu dacite

porphyry display porphyry texture and massive structure, and consists of 25% quartz, 20% feldspar and 10% plagioclase.

The porphyry Mo mineralization is hosted in the Dabaoshan granodioritic porphyry and the Chuandu granodioritic porphyry, while the skarn Mo mineralization occurred in the northeastern area, where the Jurassic Chuandu granodiorite intruded the Upper Devonian limestone (Fig.1). Besides, Xiang et al. (2015) [25] obtained the molybdenite Re–Os age of 163 Ma for the Mo porphyry deposit. All above, the Jurassic diagenetic age is consistent with the Mo porphyry metallogenic age.

2.2.3 Mineralization

The Dabaoshan deposit contains a total of 49 orebodies, including porphyry Mo, skarn Mo and strata–bound Cu–Pb–Zn orebodies. Porphyry Mo mineralization are mainly situated near the contact zone between the Dabaoshan intrusion and the Jinquling intrusion, while the others are concentrated on the northern margin of the Chuandu granodioritic intrusion (Fig. 2a). Nine porphyry ores have been discovered. The No. III orebody, as the largest one, is over 620 m in strike, 680–810 m in inclination and 42–235m in thickness, with molybdenite reserve of 116290 t at ore grades of 0.06 – 0.13 wt%.

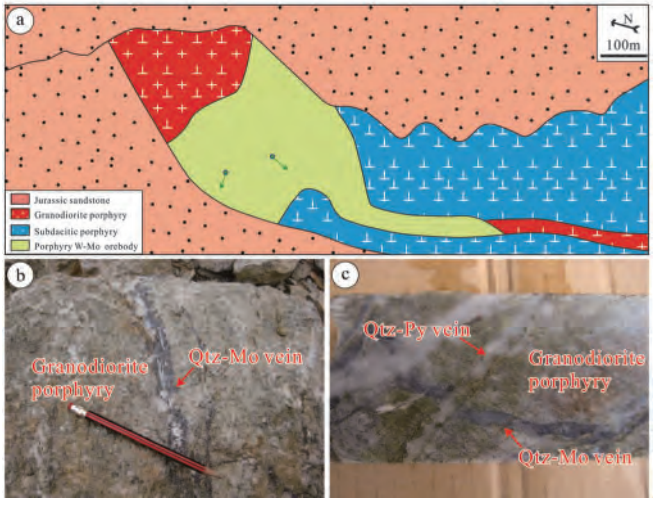

Fig.2 (a) Geologic map of cross section of the porphyry Mo deposit at Dabaoshan (modified after Zhu et al., 2011 [24]); (b) ore from porphyry Mo orebody at Dabaoshan, hosting quartz-molybdenite vein; (c) ore from porphyry Mo orebody at Dabaoshan, hosting quartz"molybdenite, cut by quartz–pyrite vein.

Skarn Mo mineralization occur in a garnet skarn zone where the Chuandu granodioritic porphyry intruded into the limestone of Tianziling formation (Fig.1). The skarn zone is 2200m long and 40m-100m thick, extending from east to west. Six lenticular-shaped skarn Mo orebodies have been discovered, with an ore grade of 0.1–0.8 wt% molybdenite.

Strata-bound Cu–Pb–Zn orebodies are hosted in the Dabaoshan dacitic porphyry and the contact zone between the Dabaoshan dacitic porphyry and the limestone of lower Donggangling formation. The mineralization zone is 3100m long and 500m thick. 33 orebodies have been discovered in the belt, being stratiform, stratoid and lenticular, and they are consistent with the altitude of the limestone layer with reserves of 0.31 Mt Cu (avg = 0.86 wt%), 20000 t of Pb (avg = 1.77 wt%) and 52000 t of Zn (avg = 4.44 wt% [26]).

The porphyry Mo orebodies are mainly composed of quartz–molybdenite and quartz-pyrite veins, with thickness ranging from a fraction of tens of millimeters. The ore minerals comprise molybdenite, pyrite, and several trace minerals, including chalcopyrite, wolframite, galena, sphalerite, rutile, while the gangue minerals consisting of quartz, K-feldspar, biotite, chlorite, muscovite and calcite.

The strata-bound Cu–Pb–Zn orebodies present three main ore types: pyrite-chalcopyrite ores, pyrrhotite-chalcopyrite ores, and galena-sphalerite ores. The ore minerals are dominated by pyrite, pyrrhotine, chalcopyrite, chalcocite, native bismuth, galena, sphalerite, limonite, and the gangue minerals include quartz, sericite, fluorite, muscovite and calcite. Cu mineralization mainly distributes in the northern area, while Pb–Zn mineralization commonly occur in the southern area.

Veins crosscutting and paragenetic minerals indicate that porphyry Mo mineralizaition can be divided into two stages, including: quartz-molybdenite stage (Stage I), quartz-pyrite stage (Stage II). Stage I is characterized by the quartz-molybdenite vein (Q1). Minerals formed at Stage I include molybdenite, rutile, pyrite, quartz, k-feldspar, apatite, calcite. Alteration halos are not well developed, but K-feldspar and minor biotite occurs along vein edges.

Stage II is characterized by the quartz-pyrite vein (Q2), which cuts Q1veins (Fig.2b, 2c), and minerals formed at Stage II include pyrite, chalcopyrite, galena, sphalerite, quartz, muscovite, chlorite and kaolinite.

3. Sampling and methods

3.1 Sampling and preparation

Based on our previous study on geology of the Dabaoshan deposit, 5 ore samples were collected from the open pit and drilling cores. Quartz-molybdenite ore with rutile were obtained from ZK6002 drilling core at 776m (DBS-1), 778m (DBS-2) and ZK5601 drilling core at 512m (DBS-3), 763m (DBS-5), and the porphyry Mo ores were collected at the contact zone between the Dabaoshan granodioritic porphyry and the Jiuquling dacitic porphyry (DBS-5).

Sample preparation includes petrographic microscopy at the key laboratory of metallogenic prediction of nonferrous metals and geological environment monitor (Central South University), Changsha, China.

3.2 Analytical methods

EPMA analysis on rutile mainly includes back-scattered

electron (BSE) observation, in-situ major elements analysis and geochemical mapping. It was carried out in the School of Geoscience and Info-Physics of the Central South University, using a EPMA–1720H (Shimadzu Corporation, Japan). The analysis was performed under the condition of accelerating voltage of 15kV, probe current of 1.0×10^{-8} A and beam size of 1μm . Natural minerals were used as standards for various elements in rutile, including quartz [Si], titania [Ti], fluorite [Ca], chromium oxide [Cr], zircon [Zr], hematite [Fe], and elemental tungsten was used as standard for [W]. The spectral lines, peak time (s), and off-peak background time (s) used for the (WDS) analysis are as follows: Si (Kα, 10, 5), Ti (Kα, 10, 5), Ca (Kα, 10, 5), Cr (Kα, 10, 5), Zr (Kα, 10, 5), Fe (Kα, 10, 5), W (Kα, 10, 5). Detection limits for all elements are below 0.01 wt%. The raw data are corrected by ZAF method using proprietary Shimadzu software. The parameters for EPMA analysis are given in Table 1.

TABLE 1 CONDITIONS OF ELECTRON MICROPROBE ANALYSIS

	SiO_2	TiO_2	CaO	Cr_2O_3	ZrO_2	FeO	WO_3
X–Ray Lines	Kα	Kα	Kα	Kα	Kα	Kα	Kα
Crystal	PET	LIF	PET	LIF	PET	LIF	PET
Standard	SiO_2	TiO_2	CaF	Cr_2O_3	ZrO_2	Fe_2O_3	W

4. Results

4.1 GEOLOGY OF RUTILE

The rutile was only observed in quartz-molybdenite veins of porphyry Mo ores under reflective lighting. The rutile is light grey, with low reflectance (lower than molybdenite but higher than apatite), slightly homogeneity and light red internal reflection. Rutile is harder than molybdenite and apatite, and the grains are mostly subhedral and anhedral. The rutile from orebodies have larger grains (approximately 100× 200 μm^2) than those from porphyry (approximately 20×15 μm^2).

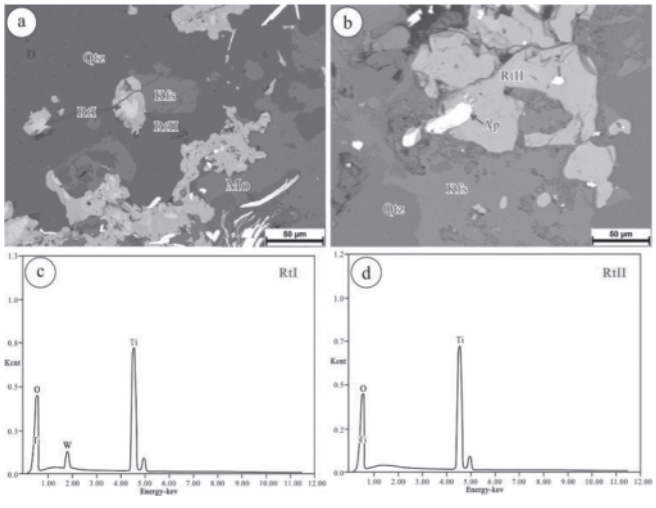

Fig.3 EDS spectrograms of rutile. (a) back-scattered electron images show discontinuous chemical zones in rutile I; (b) back-scattered election images of rutile II; (c) EDS spectrogram of brighter area in rutile I composes of Ti, O and W; (d) EDS spectrogram of rutile II compose of Ti and O. Mo = molybdenite, Rt = rutile, Ap = apatite, Kfs = K–feldspar, Qtz = quartz.

Besides, discontinuous chemical zoning in rutile from orebodies can be identified in back-scattered electron images (Fig.3a), while rutile from porphyry are less likely to be zoned, which indicates that there are two generations of rutile (rutile I and rutile II). Brighter areas in the rutile I reflect higher mean atomic number. EDS spetrograms show that not only Ti and O, but also W are hosted in the brighter areas, while no W signal have been detected in the rutile II (Fig.3c, 3d).

4.2 COMPOSITIONS OF W-BEARING RUTILE

A total of 22 spots are analyzed on six rutile grains of 3 samples (DBS-2, DBS-5, XK1), and one half of them are on rutile I and the other half are on rutile II. The spots were selected based on back-scattered electron images and X-ray element-distribution maps. The single rutile I grain is characterized by discontinuous chemical bands and heterogeneous distribution of W and Cr, and they are mainly concentrated in brighter areas (Fig.4).

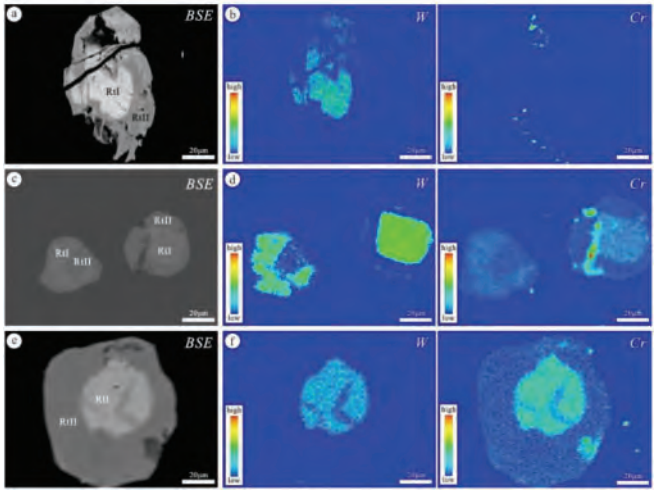

Fig.4 Back–scattered election images of rutile (a, c, e) and X"ray element"distribution maps for W and Cr of rutile (b, d, f). Rt = rutile.

Rutile I in the Dabaoshan deposit contains 0.02–0.32wt% SiO_2, 83.89–96.96 wt% TiO_2, 0.01–0.17 wt% CaO, 1.11–3.09wt% Cr_2O_3, 0.11–0.58 wt% ZrO_2, 0.17–1.55 wt% FeO, 0.23–9.57 wt% WO_3. Rutile II contains 0.01–0.21 wt% SiO_2, 94.30–98.79 wt% TiO_2, 0.01–0.05 wt% CaO, 0.06–0.18 wt% Cr_2O_3, 0.01–0.08 wt% ZrO_2, 0.57–1.68 wt% FeO, 0.14–1.53 wt% WO_3. Moreover, chemically zoned rutile I grains from high ore grade areas contain zones with 4.79-9.57 wt% WO_3 and 2.24-3.09 wt% Cr_2O_3 where biotite and K-feldspar are present as main alteration minerals.

Table 2. Representative EPMA data for rutile (%)

No.	SiO_2	TiO_2	CaO	Cr_2O_3	ZrO_2	FeO	WO_3	Total
Rutile I								
Dbs2a1	0.16	87.54	0.01	2.83	0.11	1.15	8.02	99.83
Dbs2a2	0.32	90.56	0.03	2.24	0.20	0.74	4.79	98.87
Dbs2a3	0.31	96.96	–	1.31	0.15	0.19	0.23	99.14
Dbs2a4	0.27	86.71	0.11	3.06	0.20	1.07	7.52	98.85
Dbs2a5	0.12	86.80	0.17	3.02	0.17	1.15	7.51	98.84
Dbs5a1	0.02	83.89	0.01	2.88	0.58	1.55	9.57	98.50
Dbs5a2	0.02	85.91	–	3.05	0.28	1.25	8.33	98.84
Dbs5a3	0.03	96.75	–	1.11	0.23	0.23	0.15	98.51
Dbs5a4	0.32	95.83	–	1.24	0.14	0.22	0.96	98.70
Dbs5b1	0.12	86.56	0.01	3.09	0.58	0.86	7.38	98.60
Dbs5b2	0.09	94.54	0.01	1.83	0.40	0.17	2.36	99.39
Rutile II								
XK1a1	0.12	97.77	0.05	0.14	0.07	0.79	0.52	99.45
XK1a2	0.21	95.51	0.02	0.00	0.08	1.10	1.34	98.27
XK1a3	0.07	96.79	0.00	0.11	0.06	0.87	0.64	98.53
XK1a4	0.00	97.29	0.03	0.11	0.02	0.90	1.10	99.45
XK1b1	0.01	96.43	0.02	0.08	0.01	0.87	0.98	98.40
XK1b2	0.08	96.89	0.00	0.06	0.01	1.11	1.53	99.68
XK1b3	0.09	96.71	0.00	0.10	0.02	0.91	0.98	98.80
XK1b4	0.16	96.50	0.02	0.18	0.04	0.70	0.77	98.37
XK1c1	0.03	98.23	0.02	0.06	–	0.82	0.71	99.87
XK1c2	0.04	98.79	0.00	0.08	–	0.57	0.14	99.62
XK1c3	–	95.30	0.01	0.18	0.03	1.68	1.21	98.41

Table 3 Element correlation coefficient matrix table of rutile I in the Dabaoshan deposit

	Si	Ti	Ca	Cr	Zr	Fe	W
Si	1.00						
Ti	0.28	1.00					
Ca	0.12	–0.39	1.00				
Cr	–0.31	–0.99	0.42	1.00			
Zr	–0.44	–0.46	–0.08	0.47	1.00		
Fe	–0.38	–0.95	0.31	0.91	0.39	1.00	
W	–0.36	–0.99	0.32	0.97	0.47	0.97	1.00

Table 4 Element correlation coefficient matrix table of rutile II in the Dabaoshan deposit

	Si	Ti	Ca	Cr	Zr	Fe	W
Si	1.00						
Ti	–0.34	1.00					
Ca	0.33	0.11	1.00				
Cr	–0.24	–0.56	0.03	1.00			
Zr	0.53	–0.49	0.298	0.38	1.00		
Fe	–0.14	–0.84	–0.32	0.39	0.33	1.00	
W	0.16	–0.74	–0.19	–0.17	0.083	0.70	1.00

Correlation coefficients of several elements in rutiles from the Dabaoshan deposit (Tables 2 and 3) show strongly negative correlation between Ti-Cr (–0.99), Ti-W (–0.99) in rutile I (Table 3). However, negative correlation between Ti–Cr (–0.56), Ti”W (–0.74) are less strong in rutile II (Table 4). The correlation of rutile indicates that Cr and W enter the lattice of rutile through isomorphic replacement.

5. Discussion

5.1 Genesis of rutile in the porphyry Mo ores

There are several origins of rutile including magmatic origin, hydrothermal origin, metamorphous origin and sedimentary origin. For calc-alkaline porphyry-related system, magmatic rutile is seldomly formed as an accessory mineral. However, the alteration process of hydrothermal rutile can be concluded as follows: (i) magmatic biotite alters to phlogopite, (ii) titaniferous magnetite alters to magnetite, (iii) ilmenite alters to rutile in areas of intense alteration (Sulfur-rich areas) and (iv) titanite alters to calcite in propylitic zones (mostly-Sulfur-poor but CO_2-rich areas), i.e.

(i) $K(Fe, Mg, Ti)_3(Si_3Al)O_{10}(OH)_2$ (Biotite) + S_2 = $K(Mg, Fe)_3(Si_3Al)O_{10}(OH)_2$ (Phlogopite) + FeS_2 + TiO_2

(ii) $2(Fe, Ti)_3O_4$ (Timagnetite) + S_2 = Fe_3O_4 (Magnetite) + FeS_2 + TiO_2

(iii) $FeTiO_3$ (Ilmenite) + S_2 = FeS_2 + TiO_2

(iv) $CaTiSiO_5$ (Titanite) + CO_2 = TiO_2 + $CaCO_3$ + SiO_2

As indicated above, rutile in the Dabaoshan porphyry Mo orebodies is hosted in the quartz-molybdenite veins and closely related to biotite and K-feldspar alteration. It usually distributes near biotite and K-feldspar under reflective lighting or on back-scattered electron images. Thus, the rutile from the porphyry Mo orebodies can be regarded as hydrothermal origin, and the rutile forming process can be described as follows: Ti–rich magnetic biotite showed alteration and released Ti in the hydrothermal alteration process, contributing to formation of rutile.

5.2 Factors Influencing Composition of rutile from porphyry Mo ores

Discontinuous chemical zones have been reported in

various minerals including garnet, pyrite, sphalerite and titanite, but rarely in rutile [6], especially in porphyry Mo deposit. The EPMA analysis results of rutile in the Dabaoshan porphyry Mo orebodies show that rutile I grains closer to orebodies are chemically zoned (in W and Cr), but it is less likely to be chemically zoned in rutile II further from orebodies.

Previous studies have recognized that the growth rate of crystal being faster than the cation diffusion rate in the crystal would cause discontinuous chemical zones [28], and they provided four possibilities to explain the initial anisotropic enrichment: (i) differences in growth rates on different faces[28], (ii) differences in face normal diffusion rates on different faces[29], (iii) difference in the atomic configuration of the surface on different faces[27], (iv) differences in growth mechanisms on different faces [30]. As we cannot index the prism faces, we are unable to make sure which one(s) made dominant contribution to this process. However, possibility (ii) should be one factor contributing to this process, since W^{6+} is the most highly charged yet the smallest sized cation in the rutile one. Thus, when anisotropic surface enrichment of W^{6+} occurred, its diffusion rate is slower than other cations. This gives a reasonable explanation for the discontinuous chemical zones in rutile I.

Besides, it is apparent that contents of some trace elements, including Si, Cr, Zr and W, in rutile II are lower than their counterparts in rutile I, which indicates a sudden change in chemical composition. The change is probably explained by changes in external conditions including changes in pressure, temperature, chemistry [31]. These variable changes can affect solution of trace elements, which would result in different contents of trace elements.

5.3 Processes of rutile formation during the porphyry Mo mineralization

The Dabaoshan porphyry Mo-polymetallic deposit is closely related to paleo-pacific plate subduction toward southwest, which caused lithosphere thinning, crust mantle mixing and magma forming in depthin Jurrasic[32-33]. Moreover, frequent magmatic activeties and mineralization events took place in the Nanling Metallogenic Belt under this background, with the intrusion of serveral rocks and formation of porphyry Mo, skarn Mo and strata–bound Cu–Pb–Zn orebodies in the Dabaoshan district. The porphyry Mo orebodies are closely related to the Dabaoshan and Chuandu intrusions. Previous geochemical studies show that ore–forming fluid and materials include Cu, Pb, Zn are mainly originated from the Dabaoshan granodioritic porphyry and the Chuandu granodioritic. Besides, fluid inclusion studies show that the initial ore-forming fluid was characterized by high pressure (1.9 ± 0.2 kbars), high temperature (530 ± 40□) and high oxygen fugacity [26]. Consequently, the formation of the rutile can be described as follows: ore-forming fluid migrated through fissures developed in the intrusive rocks and formed veins with biotite and K-feldspar alteration during the porphyry Mo mineralization process. Rutile I is formed firstly, closer to ores and characterized by being chemically zoned, while rutile II is formed afterward, further from ores and less likely to be chemically zoned. Besides, trace elements in rutile II are lower content than rutile I, which mainly results from sudden changes in pressure, temperature or chemistry.

5.4 Rutile indications for the porphyry Mo mineralization

Rutile is only hosted in porphyry Mo orebodies and closely related to biotite and K-feldspar alteration, which accords with high ore grade areas. As it is away from this areas, no rutile can be seen. Besides, though rutile is only found in high grade areas, it contains two generations (rutile I and rutile II). Rutile I grains closer to ores are larger (approximating to 100×200 μm^2) than rutile II grains more distal to ores (nearly 20×15 μm^2). Moreover, rutile I grains closer to ores are chemically zoned (in W and Cr), while rutile further from ores are less likely to be chemically zoned. Table 2 and Fig.5 clealy shows that rutile I grains have high W contents (4.79–9.57 wt%) and Cr contents (2.24–3.09 wt%) in coherent zones. Lastly, sometrace elements including Si, Cr, Zr and W are lower contents than rutile I. Thus, rutile in biotite and K-feldspar alteration areas together with rutile grain sizes and anomalous W, Cr and contents of most trace elements are critical indicator of economic mineralization.

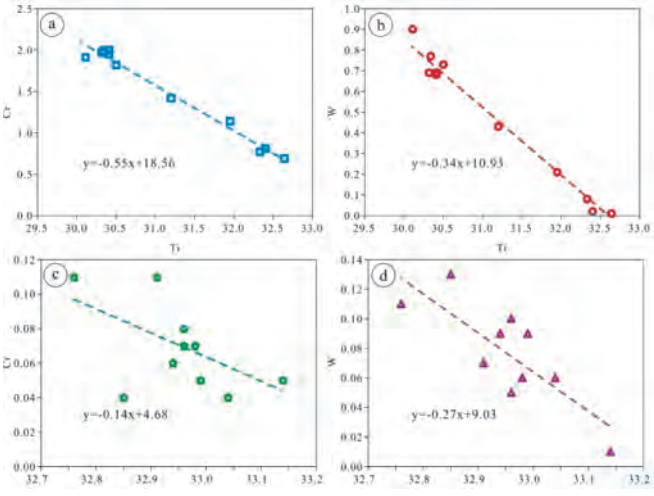

Fig.5 Correlation between trace elements and Ti in rutile from the Dabaoshan porphyry Mo ores
(a) Correlation between Cr and Ti in rutile I; (b) Correlation between W and Ti in rutile I; (c) Correlation between Cr and Ti in rutile II; (d) Correlation between W and Ti in rutile II

7. Conclusions

(1) Rutile in the Dabaoshan Mo-polymetallic deposit is only developed in the porphyry Mo ores and closely related to biotite and K-feldspar alteration, which accords with high grade areas.

(2) Rutile contains two generations (rutile I and rutile II). Rutile I is closer to ores and characterized by larger

sizes (approximating to 100×200 mm^2) and being chemically zoned (in W and Cr), but rutile II is further from ores, smaller sizes (nearly 20×15 mm^2), less likely to be chemically zoned and lower trace elements contents.

(3) EPMA analysis results show that anomalous W and Cr in coherent zones of rutile are separately 4.79–9.57 wt% and 2.24–3.09wt%.

(4) Slower diffusion rate of W^{6+} is an important factor causing chemical zones in rutile I. Changes in pressure, temperature or chemistry would result in lower contents of trace elements including Si, Cr, Zr and Ti in rutile II.

(5) Rutile in the porphyry Mo ores is formed during the hydrothermal alteration process. Thus, rutile in biotite and K-feldspar alteration areas together with rutile grian sizes and anomalous W, Cr and contents of most trace elements are critical indicator of economic mineralization.

Acknowledgment

This research is funded by the Project of Innovation-driven Plan of the Central South University (2015CX008).

References

[1] Urban A. J., Hoskins B. F., Grey I. E., (1992): "Characterization of V-Sb-W-bearing rutile from the Hemlo gold deposit, Ontario," *Canadian Mineralogist*, vol. 33, no. 3, pp. 319-326.

[2] Wan F. H., (1994): "Geochemistry and mineralogy of Ta-Nb rutile from Peninsular Malaysia," *Journal of Southeast Asian Earth Sciences*, vol. 10, no. 1-2, pp. 11-23. (in Chinese with English abstract)

[3] Brenan J. M., Shaw H. F., Phinney D. L., (1994): "Rutile"aqueous fluid partitioning of Nb, Ta, Hf, Zr, U and Th: implications for high field strength element depletions in island–arc basalts," *Earth & Planetary Science Letters*, vol. 128, no. 128, pp. 327-339.

[4] Murad E., Cashion J. D., Noble C. J., (1995): "The chemical state of Fe in rutile from an albitite in Norway," *Mineralogical Magazine*, vol. 59, no. 3, pp. 557-560.

[5] Michailidis K. M., (1996): "An EPMA and SEM study of niobian"tungstenian rutile from the Fanos aplitic granite, Central Macedonia, *Northern Greece*," N. Jb. Miner. Mh., vol. 12 pp. 549"563.

[6] Rice C. M., Darke K. E., Still J. W., Lachowski E. E., (1998): "Tungsten–bearing rutile from the Kori Kollo gold mine, Bolivia," *Mineralogical Magzine*, vol. 62, pp. 421-429.

[7] Bromiley G., Hilaret N., Mccammon C., (2004): "Solubility of hydrogen and ferric iron in rutile and TiO_2 (II): Implications for phase assemblages during ultrahigh"pressure metamorphism and for the stability of silica polymorphs in the lower mantle," *Geophysical Research Letters*, vol. 310, no. 4, pp. 373-394.

[8] Zack T., Kronz A., Foley S. F., (2002): "Trace element abundances in rutiles from eclogites and associated garnet mica schists," *Chemical Geology*, vol. 184, no. 1-2, pp. 97-122.

[9] Scott K. M., (2005): "Rutile geochemistry as a guide to porphyry Cu"Au mineralization, North parkes, New South Wales, Australia," *Geochemistry Exploration Environment Analysis*, vol. 5, no. 3, pp. 247-253.

[10] Carruzzo S., Clarke D. B., Pelrine K. M., (2006): "Texture, composition, and origin of rutile in the South Mountain Batholith, Nova Scotia," *Canadian Mineralogist*, vol. 44, no. 3, pp. 715-729.

[11] Lawrenece L.J., Savage E.N., (1975): "Mineralogy of the titaniferous porphyry copper deposit of Melanesia," *Mining Metallurgy Proc*, vol, 256, pp.1-14.

[12] Williams S. A., (1977): "Rutile and Apatite: Useful Prospecting Guides for Porphyry Copper Deposits," *Mineralogical Magazine*, vol. 41, no. 318, pp. 288-292.

[13] Czamanske G. K., Force E. R., Moore W. J., (1981): "Some geologic and potential resource aspects of rutile in porphyry copper deposits," *Economic Geology*, vol. 76, no. 8, pp. 2240-2246.

[14] Li J., Qin K., Li G., (2008): "Characteristics of rutiles from Duobuza gold"rich porphyry copper deposit in Bangong Lake Belt of northern Tibet and their significanc," *Mineral Deposits*, vol. 27, pp. 209"219. (in Chinese with English abstract)

[15] Wang L., Ming-An H. U., Yang Z., (2010): "Geochronology and Its Geological Implications of LA-ICP-MS Zircon U-Pb Dating of Granodiorite Porphyries in Dabaoshan Polymetallic Ore Deposit, North Guangdong Province," *Earth Science*, vol. 35, no. 2, pp. 175-185. (in Chinese with English abstract)

[16] Mao W., Li X., Yang F., (2013): "Zircon LA"ICP"MS U"Pb ages of granites at Dabaoshan polymetallic deposit and its geological significance, Guangdong, South China." *Acta Petrologica Sinica*, vol. 29, no. 12, pp. 4104-4120. (in Chinese with English abstract)

[17] Liu X, Zhou S., (1985): "On the occurrence of Middle Ordovician volcanics and analysis of ore"forming mechanism of siderite polymetallic deposit from Dabaoshan, Qujiang County, Guangdong province," *Journal of Nanjing University* (Natural Sciences Edition), vol. 2, no, 21, pp. 348-361,. (in Chinese with English abstract)

[18] Huang S., Zeng Y., Jia G., (1987): "On the genesis of dabaoshan polymetallic deposit in Guangdong Province, China," *Chinese Journal of Geochemistry*,

vol. 6, no. 4, pp. 322-330. (in Chinese with English abstract)

[19] Cai J., Liu J., (1993): "The age of the magmatic rocks of Dabaoshan polymetallic ore feld in north Guangdong," *Guangdong Geology*, vol. 1, no. 13, pp. 45-52. (in Chinese with English abstract)

[20] Yang Z., (1997): "Origin of the Dabaoshan massive sulfde deposit: Devonian sea-floor thermal events," *Geology and Mineral Resources of South China*, vol. 1, pp. 7-17. (in Chinese with English abstract)

[21] Xu W., Li H., Chen M., (2008): "Isotope Evidence of Material Sources of the Dabaoshan Polymetallic Deposit," *Acta Geoscientica Sinica*, vol, 6, no. 29, pp. 684-690. (in Chinese with English abstract)

[22] Wang L., Hu M., Yang Z., (2011): "U–Pb and Re–Os geochronology and geodynamic setting of the Dabaoshan polymetallic deposit, northern Guangdong Province, South China," *Ore Geology Reviews*, vol. 43, no. 1, pp, 40-49. (in Chinese with English abstract)

[23] Zhu X., Wei C., Wang Y., (2011): "Metallogenic system and prospecting prediction in the Dabaoshan Mo"W polymetallic deposit, Guangdong Province," *Mineral Exploration*, vol. 6, no. 2, pp. 661-668. (in Chinese with English abstract)

[24] Pan H., Kang Z., Fu W., (2014): "SHRIMP zircon U"Pb ages of Xuwusubdacitic porphyry in the Dabaoshan ore district of northern Guangdong Province and its geological implications," *Geological Bulletin of China*, vol, 33, no. 6, pp. 894-899. (in Chinese with English abstract)

[25] Xiang J., Liang X., Dong C., (2015): "Study on zircon U-Pb ages, molybdenite Re-Os ages and metallogenic system in the Dabaoshan W"Mo polymetallic deposit, Guangdong Province," *Journal of Jilin University* (Earth Science Edition), vol. 1, no. 45, pp. (in Chinese with English abstract)

[26] Mao W., Rusk B., Yang F., (2017): "Physical and Chemical Evolution of the Dabaoshan Porphyry Mo Deposit, South China: Insights from Fluid Inclusions, Cathodoluminescence, and Trace Elements in Quartz," *Economic Geology*, vol. 112, no. 4, pp. 889-918. (in Chinese with English abstract)

[27] Nakamura Y., (1973): "Origin of sector-zoning of igneous clinopyroxenes," American Mineralogist, vol. 58, pp. 986-990.

[28] Downes M. J., (1974): Sector and oscillatory zoning in calcic augites from M. Etna, Sicily," Contributions to Mineralogy & Petrology, vol. 47, no. 3, pp, 187-196.

[29] Larsen L. M., (1981): "Sector zoned aegirine from the Ilímaussaq alkaline intrusion, South Greenland," Contributions to Mineralogy & Petrology, vol. 76, no. 3, pp. 285-291.

[30] Watson E. B., Liang Y. A., (1995): "simple model for sector zoning in slowly growing crystals: Implications for growth rate and lattice diffusion, with emphasis on accessory minerals in crustal rocks," American Mineralogist, vol, 80, no. 1-2, pp. 1179-1187.

[31] Kouchi A., Sugawara Y., Kashima K., (1983): "Laboratory growth of sector zoned clinopyroxenes in the system $CaMgSi_2O_6$ "$CaTiAl_2O_6$," Contributions to Mineralogy & Petrology, vol. 83, no. 1-2, pp. 177-184.

[32] Yardley B. W. D., (1991): "Oscillatory Zoning in Metamorphic Minerals: An Indicator of Infiltration Metasomatism," *Mineralogical Magazine*, vol. 55, no. 380, pp. 357-365.

[33] Mao J., Chen M., Yuan S., (2011): "Geological Characteristics and Time-Space Distribution Regularities in the Qinzhou–Hangzhou Metallogenic Belt in South China," *Acta Geologica Sinica*, vol. 5, no. 85, pp. 636-658.

[34] Liu S., Wang C., Huang W., (2012): "LA"ICP"MS Zircon U-Pb ages and Dynamic Background of the Dabaoshan Porphyry Associated with Mo"W Mineralization in Northern Guangdong Province," *Geotectonica et Metallogenia*, vol. 3, no. 36, pp. 440-449. (in Chinese with English abstract)